The Impact of Action Potential and Conduction Velocity Distribution Changes on Markers of Repolarization Dispersion

[1]G. Kozmann, [1]G. Tuboly, [2]V. Szathmáry, [3]J. Švehlíková, [3]M. Tyšler

[1]Department of Electrical Engineering and Information Systems, Faculty of Information Technology, University of Pannonia, Veszprém, Hungary,
[2]Institute of Normal and Pathological Physiology, Slovak Academy of Sciences, Bratislava, Slovakia,
[3]Institute of Measurement Science, Slovak Academy of Sciences, Bratislava, Slovakia
Email: kozmann.gyorgy@virt.uni-pannon.hu

Abstract. *A necessary prerequisite of malignant arrhythmias is the elevated repolarisation dispersion (RD) of the ventricular myocardium. In this study, by the use of numerical heart and thorax models the RD properties were analyzed as a function of realistic action potential duration (APD) and activation propagation velocity (CV) changes taken from recent experimental studies of normal and heart failure cases. The contribution of APD and CV variability to the arrhythmogenic substrate of malignant arrhythmias was studied separately and in combination. RD was quantitatively characterized by the analysis of computer simulated QRST integral maps and non-dipolarity indices. Modelling study revealed that transmural APD variability is primarily responsible for the arrhythmogenic substrate. Depending on the transmural gradient, CV may moderate or enhance the resultant repolarization heterogeneity level.*

Keywords: Malignant Arrhythmias, Repolarization Dispersion, Numerical Heart and Thorax Models, QRST integral maps, Transmural Gradient

1. Introduction

Ventricular tachycardia and fibrillation are the most common causes of sudden cardiac death (SCD). In spite of the continuous development of risk assessment methods, still no reliable ECG based marker of arrhythmia prone status does exist according to the scientific statement of the AHA/ACCF/HRS based on hundreds of clinical trials [1]. According to theoretical expectations, parameters casually reflecting the spatial heterogeneity of the elementary myocardial volumes might be the clue of a more efficient risk assessment [2].

In this study we attempted to link the observed normal and pathological QRST integral – and non-dipolarity index (NDI) – behaviour, to mesoscopic (intramural) and even to microscopic experimental findings. To this end, numerical chest and multi-element heart models were used. In the heart model, action potential duration (APD) and activation propagation velocity (CV) values of the different myocardial layers were approximated based on the recent optical mapping results of stained subepicardial, midmyocardial and subendocardial sections taken from healthy and failing human hearts (Glukhov et al. [3]).

2. Subject and Methods

Numerical Modelling of the Heart and Thorax
A five-layer numerical heart model was used with globally or locally adjustable intramural APD and CV modulation features. In the simulations transmural gradient (TG) of epicardial and endocardial layers was defined as $APD_{epi} - APD_{endo}$. However, while keeping TG

constant, local intramural APD deviations were allowed. Similarly, different intramural CV values were allowed, expressed in modelling distance unit/modelling time unit (mdu/mtu). Finally, a piecewise realistic shape, piecewise homogeneous thoracic model was used to compute body surface potential distributions, QRST integral maps and NDIs.

Details of the simplified computer model of the human cardiac ventricles were described previously by Szathmáry and Osvald [4].
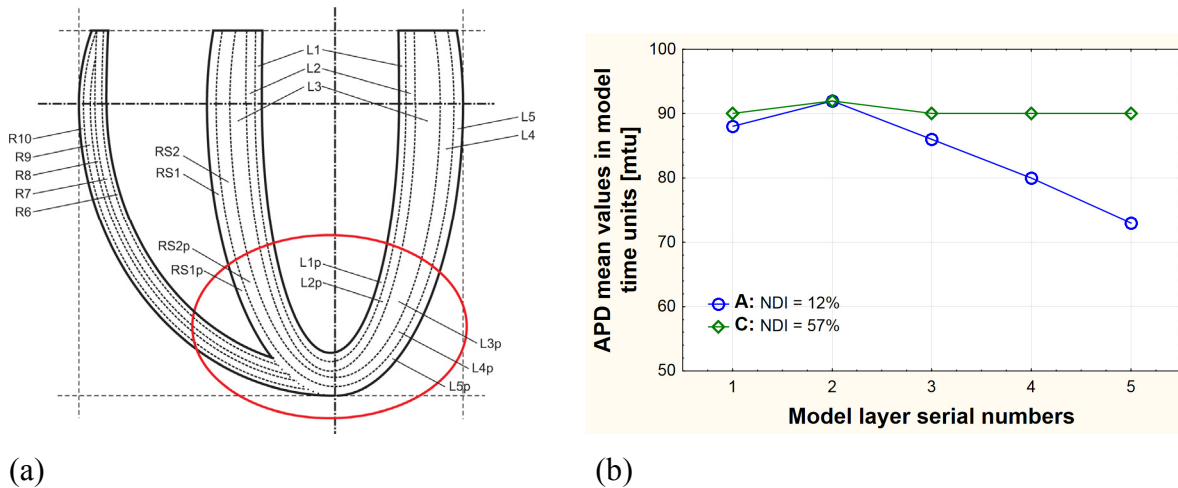

(a)   (b)

Fig. 1.   (a) A schematic representation of the "layered" structure and geometry of the left and right ventricles. In our study the ellipse at the apex contains the model region with pathologically modulated APD and CV. (b) Mean value of the APD profile of a healthy subject (profile 'A') and the failing heart profile of the apical region. The simplified graph is based on the experimental data of Glukhov et al. [3].

To compute the cardiac potentials as well as the QRST integral maps on the thoracic surface, the multiple-dipole cardiac generator has been inserted into the realistically shaped piecewise homogeneous torso model (Fig. 2).
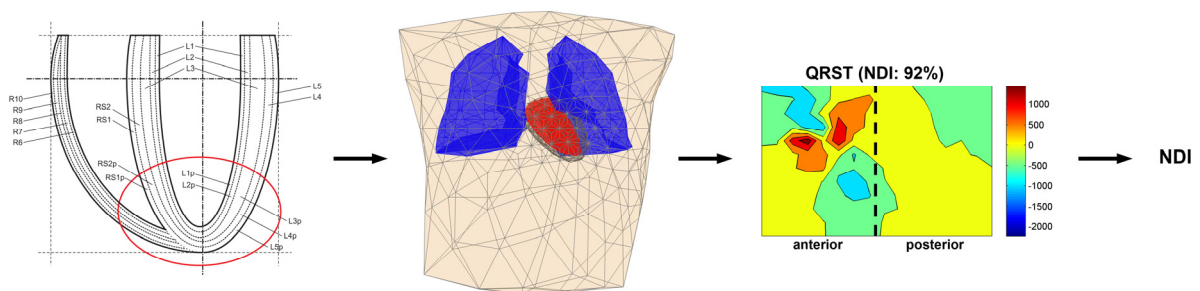

Fig. 2.   Layout of the major modelling steps.

Evaluation of Repolarization Dispersion by QRST Integrals and Non-dipolarity Indices
In a concise way QRST integral maps are characterized by the beat-to-beat sequence of NDI(QRSTint), based on the c_i components of the KL expansion:

$$NDI(QRSint) = \frac{\sum_{i=4}^{12} c_i^2}{\sum_{i=1}^{12} c_i^2} = \frac{P_{ND}}{P_D + P_{ND}} \cdot 100\% \qquad (1)$$

where NDI(QRSint)   non-dipolarity index of the QRST integral
c_i i. component of the KL expansion
P_D QRST integral map power represented by the "dipolar" KL components (i: 1-3)
P_{ND} QRST integral map power represented by the "non-dipolar" KL components (i: 4-12) according to Lux et al. [5].

3. Results

In our reference case TG was -15 mtu (modelling time unit), yielding an NDI of 16%. By the systematic change of TG in the apical part of the heart model from -15 mtu up to +14 mtu, the NDI did change from 16% up to 76%. In the reference case CV was 3 mdu/mtu in the Purkynje layer and 1 mdu/mtu in all the others. In the pathological case CV pattern was 2 mdu/mtu in the Purkynje layer, and 0.5 mdu/mtu in all the others. The NDI range due to the combined APD and CV modulations did not change, however the TG of the maximal NDI shifted slightly in the direction of positive TGs. An increase of NDIs occurred at TGs significantly positive. However the increase of APD profile slope finally caused a quick decrease of NDI. According to our modelling results uneven CV profiles between the limits shown in Fig. 3(a) resulted in NDI characteristics running between the two graphs shown in Fig. 3(b).
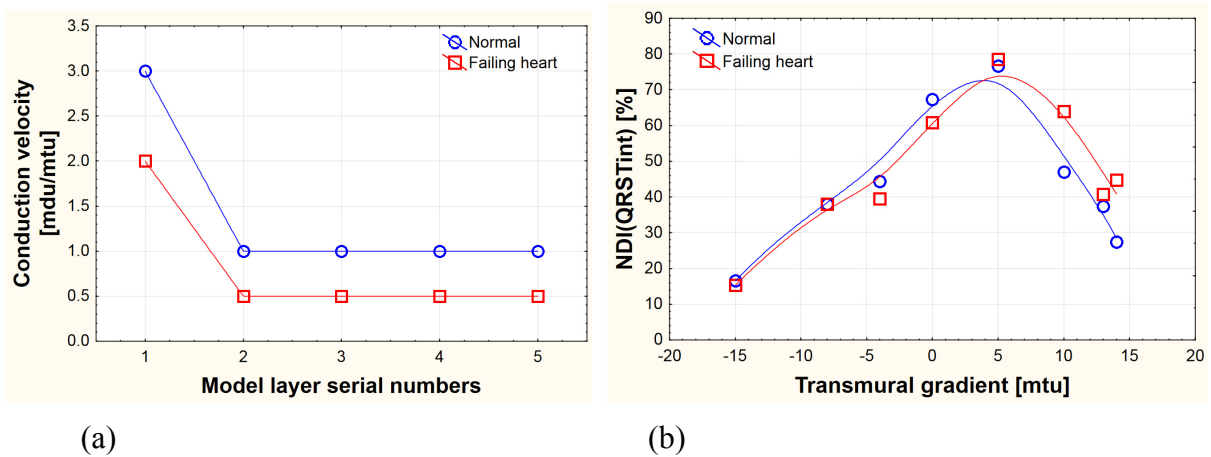

(a)   (b)

Fig. 3.   (a) Transmural CV and the NDI(QRSint) vs. TG patterns. Circle markers represent the profiles in the healthy myocardium, while square markers indicate the profiles in failing heart (apical) regions. (b) NDI(QRSint) vs. transmural gradient. Circle markers represent the relationship if CV is normal, square markers show the consequences of apical CV modulation depicted in Fig. 3(a).

A few examples of the impact of TG modulation (without CV modulation) are illustrated by the QRST integral maps shown in Fig. 4.

QRST integral (TG = -15, NDI = 17%)   QRST integral (TG = 0, NDI = 67%)   QRST integral (TG = 14, NDI = 27%)
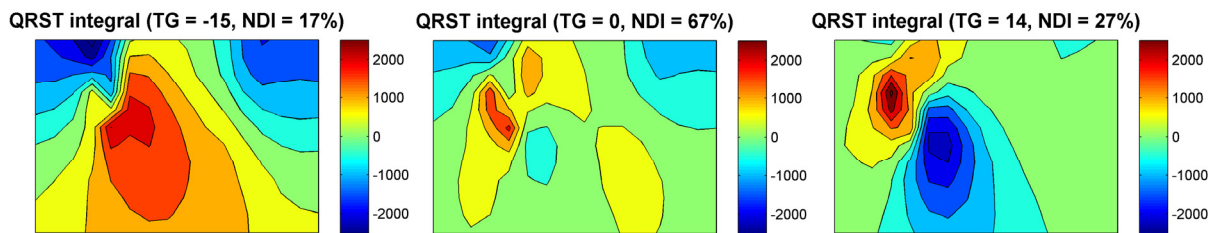

Fig. 4.   Simulated QRST integral maps vs. TG. The subsequent modulation of TG results the most fragmented QRST integral pattern at the transition of TG from negative into positive value. The smallest range of amplitudes are at TG = 0.

4. Discussion

According to this model study, NDI is primarily affected by the TG value. The impact of intramural local maxima/minima on RD is negligible. The impact of decreasing CV is modest until TG is negative (i.e. close to the normal APD distribution), however at TG > 0 NDI increase is more emphasized. We should remark, that positive TG slopes > 5 mdu/mtu surpass the gradients were not found in the paper of Glukhov, possibly because physically they are not possible in failing heart myocardial tissue.

The study of QRST integral maps vs. increasing TG revealed, that after reaching the NDI maximum the map pattern turned to be more and more dipolar but with reversed polarity.

Acknowledgements

References

[1] Goldberger JJ et al: A scientific statement from the American Heart Association Council on Cardiology Committee on Electrocardiography and Arrhythmias and Council on Epidemiology and Prevention. *Circulation*, 118: 1497-1518, 2008.

[2] Geselowitz DB. The ventricular gradient revisited: relation to the area under the action potential. *Biomedical Engineering, IEEE Transactions on*, (1): 76-77, 1983.

[3] Glukhov AV, Fedorov VV, Lou Q, Ravikumar VK, Kalish PW, Schuessler RB, Moazami N, Efimov IR. Transmural dispersion of repolarization in failing and nonfailing human ventricle. *Circulation research*, 106 (5): 981-991, 2010.

[4] Szathmáry V, Osvald R. An interactive computer model of propagated activation with analytically defined geometry of ventricles. *Computers and biomedical research*, 27 (1): 27-38, 1994.

[5] Lux RL, Evans AK, Burgess MJ, Wyatt RF, Abildskov JA. Redundancy reduction for improved display and analysis of body surface potential maps. I. Spatial compression. *Circulation Research*, 49 (1): 186-196, 1981.